AGU PUBLICATIONS

Water Resources Research

RESEARCH ARTICLE

10.1002/2016WR019010

Key Points:

- Regrass on steep croplands can not only reduce soil erosion but also trap eroded soil from uplands
- Raindrop impact strengthens sediment delivery, but limitedly affects sediment particle selectivity and overland flow hydraulics
- Both raindrop kinetic energy and stream power available for surface soil contribute to sediment delivery in net deposition areas

Correspondence to:
C. Pan,
pancz@bnu.edu.cn

Citation:
Pan, C., L. Ma, and J. Wainwright (2016), Particle selectivity of sediment deposited over grass barriers and the effect of rainfall, *Water Resour. Res.*, *52*, 7963–7979, doi:10.1002/2016WR019010.

Received 1 APR 2016
Accepted 21 SEP 2016
Accepted article online 27 SEP 2016
Published online 18 OCT 2016

Particle selectivity of sediment deposited over grass barriers and the effect of rainfall

Chengzhong Pan[1], Lan Ma[2], and John Wainwright[3]

[1]Key Laboratory of Water Sediment Sciences, College of Water Sciences, Beijing Normal University, Beijing, China, [2]College of Soil and Water Conservation, Beijing Forestry University, Beijing, China, [3]Department of Geography, Durham University, Durham, UK

Abstract Particle selectivity of the sediment deposited over vegetative barriers is of importance to predict sediment transport and particulate pollutant load into surface waters. Grassed barriers with 20–90% covers at 15° slope were subjected to silt-laden inflows in the presence and absence of simulated rainfalls to investigate the sediment deposition processes. The results show that regrass of steep croplands can effectively trap eroded sediment from upslope, and the rowed grass barriers can strengthen sediment deposition. The deposition order of sediment particle sizes (μm) follows ($>$50) $>$ (25–50) $>$ (10–25) $=$ ($<$2) $>$ (2–10), and the particle selectivity weakens with increasing grass covers. Clay particles had a similar deposition efficiency to overall sediment, implying the effectiveness of regrass in controlling soil nutrient loss. The contribution of grass to total overland flow resistance is almost equivalent to the percentage of grass cover. For steep grassed slopes, raindrop impact significantly decreases sediment deposition, but limitedly affects particle selectivity of deposited sediment and overland flow hydraulics. Both raindrop kinetic energy and stream power available for surface soil contribute to sediment deposition in net deposition areas of grass barriers. These imply that rainfall effect on sediment delivery over vegetated barriers derives from the additional raindrop energy, rather than the variation in runoff hydraulics. These results can help to clarify the effect of raindrop impact on sediment transport and to evaluate the benefit of revegetation in decreasing sediment yield and its particulate nutrient load into surface waters.

1. Introduction

It is well known that vegetation reduces the impact energy available for hillslope erosion from raindrops and overland runoff, and changes sediment particle transport pattern [*Parsons et al.*, 1994; *Cerdà*, 1998b; *Martinez-Mena et al.*, 2000; *Wainwright*, 2009]. In order to control soil erosion and improve eco-environment, China government implemented the "Grain for Green" project in 1999, and the cropland steeper than 15° was recommended to be revegetated as grass or forest lands [*Tang et al.*, 1998; *Deng et al.*, 2012]. In the hilly Loess Plateau with serious soil erosion, a typical cultivated hillslope is characterized as a steep convex slope and its up-to-down slopes commonly increase from 5 to 25° [*Jiang*, 1997]. Consequently, grass strips or barriers were widely restored on the steep downslope, and croplands remained on the upslope. The grass slopeland can not only decrease soil detachment but also trap the upslope eroded sediment or trigger more sediment deposition [*Pan et al.*, 2011; *Palacio et al.*, 2014], and the deposition effect even plays a dominant role in controlling soil erosion [*Pan et al.*, 2006, 2011]. Therefore, it is important to evaluate the effectiveness of regrass on steep hillslopes in reducing soil and nutrient losses into rivers for the reasonable use and protection of slopelands.

Particle size characteristics of sediment are necessary for predicting its transport process on hillslopes [*Flanagan and Nearing*, 2000; *Malam Issa et al.*, 2006; *Wainwright et al.*, 2008; *Shi et al.*, 2012], and they can suggest a guideline for controlling the off-site effects of sediment-bounded nutrients or pollutants in surface waters [*Meyer et al.*, 1980; *Turnbull et al.*, 2010; *Novara et al.*, 2013]. Many investigations have shown that fine soil particles are prone to transport in overland runoff, and coarse particles or aggregates are easily deposited on the downslope due to the greater settling velocities [*Hairsine and Rose*, 1992; *Malam Issa et al.*, 2006]. The effect of vegetation on sediment particle transport depends on soil properties, slope landforms, raindrop and runoff impacts [*Prosser et al.*, 1995; *Cerdà*, 1998a; *Martinez-Mena et al.*, 2000, 2002; *Wainwright*, 2009], and so far there is not a consistent viewpoint on the particle selectivity. For instance, *Martinez-Mena* *et al*. [2000] suggested that vegetation hampered the breakdown of soil aggregates and reduced transport of sand, and the clay and sand particles had a depletion in exchange for an enrichment in silt. However, *Zhang et al*. [2011] concluded that the vegetation cover had little effect on the particle selectivity of eroded sediment, and the runoff sediment had a greater fraction of clay and silt compared to the soil material.

When sediment-laden flow passes across an vegetated area, a reduction in the sediment load forms a net deposition [*Hairsine et al*., 2002]. There may exist differences in sediment delivery and particle selectivity between in net deposition and detachment areas due to alterations in runoff and sediment dynamics [*Beuselinck et al*., 2002; *Hairsine et al*., 2002]. The sediment deposition depends on vegetation type, width, density or cover, spatial distribution, slope steepness, and inflow sediment properties [*Liu et al*., 2008; *Gumiere et al*., 2011]. *Pan et al*. [2010] found that the removal of grass canopies had little effect on sediment deposition and the particle selectivity, and highlighted the importance of stems. More coarse particles were prone to deposition over vegetative areas, but the relationship between vegetation cover and particle selectivity of deposited sediment is still pending [*Wainwright et al*., 2008; *Pan et al*., 2010].

Raindrop impact tends to strengthen soil detachment and transport [*Savat*, 1977], and the effect weakens with the increasing water depth and slope steepness [*Guy et al*., 1990; *Kinnell*, 1991]. Raindrop impact on sediment particle transport on a hillslope can derive from an alteration to overland flow hydraulics or/and the additional raindrop kinetic energy, but it still lacks experimental observations to support the relative importance [*Hairsine and Rose*, 1992; *Zhang et al*., 2011; *Ma et al*., 2013]. In general, the information about the relationship between raindrop impact and sediment particle deposition was limited, and the exceptions in the literature were the studies of *Beuselinck et al*. [2002] and *Ma et al*. [2013]. They, respectively, used a flume bed with low slopes (i.e., 1 and 2%) and a sandpaper surface erecting plastic grass clusters to simulate the areas of sediment net deposition, and suggested that the presence of raindrop impact triggered the delivery of more coarse sediment. However, the investigations were difficult to mirror sediment deposition over vegetated slopes due to the difference in soil surface roughness and microtopography. Meanwhile, vegetation cover not only increases hydraulic resistance to overland flow but also attenuates rainfall kinetic energy impacting surface soil [*Prosser et al*., 1995; *Pan and Shangguan*, 2006; *Wainwright*, 2009]. The interaction of vegetation cover and raindrop impact leads to a greater uncertainty in predicting sediment transport on vegetated slopes [*Parsons et al*., 1994; *Morgan et al*., 1998].

This investigation aimed at the effectiveness of the regrassed steep slopes in controlling upslope inflow sediment and particle transport in the loess plateau of China. The detail objectives are (1) to clarify particle selectivity of the sediment deposited within steep grassed barriers; (2) to reveal the effects of raindrop impact and vegetation cover on the particle selectivity; and (3) to illustrate the impacting mechanism of raindrops on the sediment deposition. These results can help to understand sediment particle transport on steep vegetated hillslopes and to evaluate the benefit of the "Grain for Green" program in decreasing sediment yield and particle-bounded nutrients into surface waters.

2. Materials and Methods

2.1. Experimental Setups

The experiments were carried out in an indoor rainfall simulator hall. Ten steel trays were constructed to contain soil and establish grass plots with different covers. The tray size was 2.0 m long, 0.55 m wide, and 0.35 m deep. Some apertures were formed at the bottom of a tray to allow soil moisture to freely infiltrate. A metal runoff collector was set at the bottom of a tray to direct runoff into a container. Each tray was arranged on a removable handcart and the tray slope can be adjusted from 0° to 25° (Figure 1).

The grass barriers were subjected to silt laden inflow in the absence and presence of simulated rainfalls. The simulated rainfalls were provided by a continuous-spray system. The raindrops were formed by the horizontally opposite two spray nozzles, and naturally fell to the ground with a falling height of 16 m. The rainfall intensities were adjusted by the nozzle size and water pressure. The rainfalls had similar drop-size distributions and kinetic energies to those of natural storms in the loess hilly region [*Xu et al*., 2006; *Wang et al*., 2005].

The silt-laden inflow was provided by a mixture of water with soil, which was continuously mixed using an electric stirring system. The slurry was filled in a tank and it had a 4.0 m height water head. The slurry was first introduced to a regulating sink at the top of a grass plot, and then flowed over a grass barrier (Figure 1).

Figure 1. Experimental schematic design and grass barriers (C20, C40, C60, C70, and C90 correspond to 20, 40, 60, 70, and 90% grass covers, respectively).

2.2. Experimental Treatments

A sandy loam soil, taken from the loess hilly region, was used to fill the trays and to produce the silt-laden inflows. This is a typical loessial soil with a high concentration of silt particle (0.002–0.02 mm) and porous structure. The used soil is erodible and it partly explains the high sediment concentration in the Yellow River. The soil median particle diameter (d_{50}) was 13 μm, and the percentage by weight of particles in size ranges of <2 μm, 2–10 μm, 10–25 μm, 25–50 μm, and >50 μm were 11, 31, 29, 20, and 9%, respectively.

A 30 cm depth soil layer was packed in each tray to obtain a bulk density of 1.2 g cm^{-3}, and Perennial black rye (*Lolium perenne* L.), a local grazing grass, was sowed in the soil tray to represent the grass barrier. The grass plots had five planting densities with two replicates, and their plant and row spaces were 20 cm × 20 cm, 15 cm × 15 cm, 10 cm × 15 cm, 10 cm × 10 cm and 5 cm × 20 cm, respectively. When the grass barriers in the removable handcarts had naturally grown outdoors for 2 years, they were moved in a laboratory hall and subjected to silt-laden inflows and simulated rainfalls. At this moment, the grass barriers, respectively, corresponded to 20, 40, 60, 70, and 90% covers (Figure 1), and their dry weights of aboveground biomass increased from 142 to 516 g m^{-2} with increasing covers. Meanwhile, moss, a ubiquitous biological soil crust in the hilly loess region, was naturally grown on soil surface of each grass plot, and its depth was approximately 0.5 mm (Figure 1). Moss tended to protect the soil surface and prevent soil erosion occurrence, and the grass strips could be regarded as net deposition areas [*Pan et al*., 2006, 2010].

All grass barriers were subjected to silt-laden inflows, and raindrop impact on sediment deposition was comparably analyzed between these collected data in the presence and absence of rainfalls (Table 1). In total, 20 trials were carried out at a 15° slope under the high (H) and low (L) inflows (Table 1). The experiments design originated from the typical "up-to-down" hillslope in the hilly Loess Plateau. The experimental slope of grass barriers corresponds to a threshold slope (i.e., 15°) for the "Grain for Green" project. The low (L) and high (H) inflows, respectively, corresponded to flow rates of 15 and 30 L min^{-1} m^{-1}, and sediment

Table 1. Characteristics of the Sediment Deposited Over Grass Barriers and the Effect of Rainfall (Test L and H Represent Low and High Inflow Runs, Respectively; The Number is Grass Cover (%); R and NR Refer to the Presence and Absence of Rainfall, Respectively; as the Same Below)

Test	Covers (%)	Flow Rate[a] ($cm^2\ s^{-1}$)	Sediment Concentration ($kg\ m^{-3}$)	Sediment Delivery Rate ($g\ s^{-1}$) Inflow	Outflow	Deposited Sediment Load ($g\ m^{-2}$)	SDE (%)
L20_NR	20	2.16	23.79	2.83	2.50	435	11.7a[b]
L20_R	20	2.65	22.37	2.88	2.65	308	8.2b
L40_NR	40	2.47	24.25	3.29	2.82	618	14.4a
L40_R	40	2.58	23.30	2.92	2.66	334	8.8b
L60_NR	60	2.31	23.32	2.96	2.51	595	15.3a
L60_R	60	2.48	21.90	2.63	2.36	344	10.0b
L70_NR	70	2.61	24.10	3.46	2.77	905	20.0a
L70_R	70	2.85	22.77	3.19	2.83	470	11.2b
L90_NR	90	2.27	24.40	3.04	1.68	1790	44.9a
L90_R	90	2.44	24.00	2.82	1.80	1332	36.1b
H20_NR	20	4.85	35.89	9.57	8.75	708	8.5a
H20_R	20	5.30	31.39	8.36	8.27	72	1.0b
H40_NR	40	5.44	29.75	8.90	7.70	1047	13.5a
H40_R	40	4.76	31.61	7.48	6.84	557	8.5b
H60_NR	60	5.37	28.32	8.36	7.01	1184	16.2a
H60_R	60	6.02	26.62	8.15	7.43	623	8.8b
H70_NR	70	5.12	36.20	10.19	8.71	1294	14.5a
H70_R	70	5.16	32.74	8.48	7.60	764	10.3b
H90_NR	90	4.99	38.80	10.66	7.59	2672	28.7a
H90_R	90	5.81	35.50	10.46	7.40	2665	29.2a

[a]Flow rates include the rainfall component.
[b]The same letter represents that rainfall impact has no significant ($p = 0.05$) effect on sediment deposition efficiency (SDE) for the same cover barrier using paired t test method.

concentrations of 23.0 and 35 kg m^{-3} under the rainfall intensities of 60 and 90 mm h^{-1}. The inflow sediment parameters corresponded to the runoff and erosion characteristics on a typical upslope cropland under the given rainfalls, and the cropland commonly had a 30 m slope length, 5–10° steepness and a 0.5 mm min^{-1} soil steady infiltration rate [*Jiang*, 1997]. The 60 and 90 mm h^{-1} rainfalls, respectively, corresponded to the storm recurrence periods of 4 and 10 years in this region, but they frequently occurred on a small watershed due to the spatial variability of rainfall and were primarily responsible for soil erosion [*Jiang*, 1997]. They, respectively, generated raindrop kinetic energies of 0.25 and 0.38 J m^{-2} s^{-1}, and median raindrop diameters of 1.56 and 1.68 mm [*Wang et al*., 2005]. The low and high runs had test durations of 25 and 15 min, respectively, and the duration ensures that each trial had an almost constant outflow during the final phases of runoff.

2.3. Data Measurements and Analysis

In order to alleviate the effect of soil infiltration on runoff and sediment processes, each plot was subjected to a pilot rainfall. The pilot rainfall lasted approximately 20 min for each trial and generated a constant outflow rate. During the experiment process, the travel times across a flow line distance of 1.0 m were recorded using a stopwatch according to the propagation of dye tracer ($KMnO_4$) front, and nine measuring lines were averaged to represent *Vs* for a plot. Due to the influence of preferential surface flow, surface velocity (*Vs*) multiplied by a correction factor (α) obtains mean velocity (*V*).

$$V=\alpha \cdot Vs, \tag{1}$$

where α is less than 1.0. The α value was assigned as 0.67 in this study based on the laminar flow regimes [*Horton et al*., 1934].

Outflow runoff samples were collected at 2 min intervals to calculate runoff rate and sediment delivery rate, and a sample was collected for 1 min for low run and 30 s for high run. The difference in sediment yield between inflow and outflow was used to calculated deposited sediment load. Sediment deposition efficiency (SDE) was defined as the ratio of the deposited sediment to inflow sediment, and it can be expressed as equation (2)

$$SDE=\frac{SDR_{inflow}-SDR_{outflow}}{SDR_{inflow}}\times 100\%, \quad (2)$$

where SDR_{inflow} and $SDR_{outflow}$ are sediment delivery rates of the inflow and outflow, respectively.

Particle size distributions of the inflow and outflow sediment were analyzed by a MS2000 Laser Size Classifier (Malvern, UK). Distilled water was selected as disperser, and the dispersion time, sonication activated, agitation speed and pump speed were ascertained as 3 min, 40,800 r min^{-1}, and 2200 r min^{-1} based on pilot experiments. All sediment samples were analyzed for "ultimate" size distribution which relates to the individual primary mineral particles [*Martinez-Mena et al*., 2002].

Sediment deposition efficiency of a given particle size (SDE_{size}) is expressed as equation (3)

$$SDE_{size}=\frac{SDR''_{inflow}-SDR''_{outflow}}{SDR''_{inflow}}\times 100\%, \quad (3)$$

$$SDR''_{inflow}=SDR_{inflow}\times W_{inflow}, \quad (4)$$

$$SDR''_{outflow}=SDR_{outflow}\times W_{outflow}, \quad (5)$$

where SDR''_{inflow} and $SDR''_{outflow}$ are sediment delivery rates in a given particle size (e.g., <2 μm) of the inflow and outflow, respectively; W_{inflow} and $W_{outflow}$ is the mass percentage of the grain size fraction, and the W_{inflow} values of <2, 2–10, 10–25, 25–50, and >50 μm particles are, respectively, 11, 31, 29, 20, and 9% according to the grain size distribution of the used soils, and the $W_{outflow}$ values were provided by particle analysis of the outflow sediment samples.

Due to the same dimension with raindrop kinetic energy, unit stream power is used to describe the sediment transport, and it can be also described by multiplying shear stress and mean velocity for overland flow [*Bagnold*, 1966]

$$\omega=\rho gqS=\tau V, \quad (6)$$

where ω is unit stream power (J m^{-2} s^{-1}), ρ is the density of water (kg m^{-3}), q is unit flow rate (m^2 s^{-1}), S is slope steepness (m m^{-1}), V is mean velocity (m s^{-1}), and τ is shear stress (N m^{-2}).

For a grassed plot, τ can be separated into two components, i.e., τ_b and τ_g, respectively, impacting bed (soil) surface and grass cover [*Prosser et al*., 1995]. Consequently, ω can also divided into two components as equation (7)

$$\omega==(\tau_b+\tau_g)V=\omega_b+\omega_g, \quad (7)$$

where ω_b and ω_g are the energies dissipated by bed sediment transport and by grass stems, respectively, and ω_b can be of importance to predict sediment deposition. Assuming that τ_b can be separated from τ_g by calculating the relative contribution of the bed and grass stems toward total flow resistance [*Rauws*, 1988; *Prosser et al*., 1995], ω_b can be calculated using equation (8)

$$\omega_b=\tau_b V=\tau\left(\frac{f_b}{f}\right)V, \quad (8)$$

$$f=8gSq/V^3, \quad (9)$$

where f is Darcy-Weisbach resistance coefficient and f_b is the resistance component derived from bed surface. In this study, f and f_b were calculated using equation (9), and the V values equaled to mean flow velocities on the grassed plots and on bare soil surfaces (i.e., grass cover $C=0$), respectively.

The effects of grass cover and rainfall on runoff hydraulics and sediment deposition were analyzed using ANOVA or paired t test. Log-transformed linear regression was used to fit the runoff-sediment relationship and to discuss the particle size selectivity of sediment deposited over the grass barriers.

3. Results and Discussions

3.1. The Effect of Rainfall on Sediment Deposition

As grass cover increased from 20 to 90%, SDE increased from 8.2 to 44.9% for low (L) run, and from 1.0 to 29.2% for high (H) run (Table 1). SDE increased with increasing grass covers as an exponential function, and there were clear differences in the fitted curves (Figure 2).

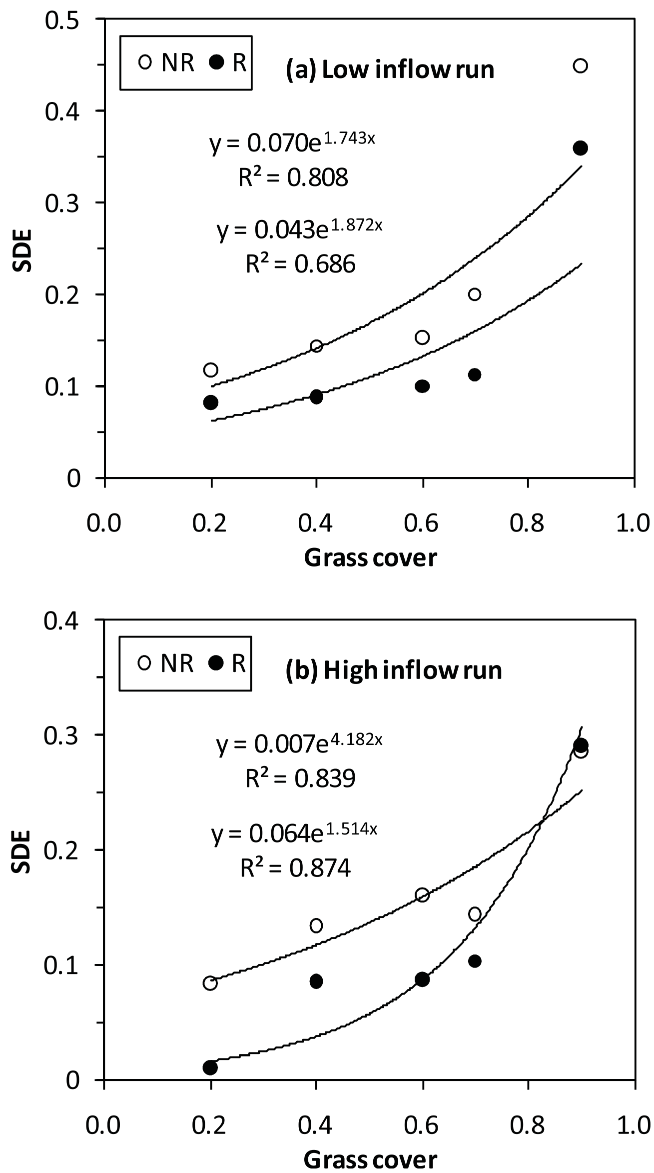

Figure 2. The relationship between sediment deposition efficiency (SDE) and grass covers and the effect of rainfall.

The 90% cover had a significantly ($p = 0.05$) greater SDE than 20–70% covers, and a minor difference in SDE existed among the 20–70% covers. This may be related with the grass clusters distribution with horizontal rows (perpendicular to flow lines) for the 90% cover (Figure 1). In this study, we found that for the scattered grass clusters (i.e., the low covers) sediment was mainly deposited in depressions on plot surface or within grass barriers, but for the rowed strips (i.e., the 90% cover) much sediment was trapped before each grass strip. The backwater zones were easily formed before the rowed grass strips, and they tend to trigger more sediment deposition [*Ma et al.*, 2013]. The considerable sediment deposition indicates that it is effective to establish grass barriers on steep downslope to control erosion sediment from upslope cropland in the loess plateau. The better performance of the rowed grass barriers implies that grass plantation with horizontal rows could be highly recommended rather than vegetation self-restoration with scattered clusters. The mode of croplands on upslope and grass on downslope remains considerable arable land, and it ensures that the local region can be self-sufficient in food. This mode should also be generalized to other similar hilly regions with steep slopes confronted by soil erosion.

ANOVA showed that rainfall impact significantly ($p = 0.05$) decreased SDE with the exception of 90% cover for high run (i.e., H90_NR and H90_R, Table 1). The reduction percentages ranged from 20 to 44% for low inflow run and from 29 to 88% for high run, and they significantly negatively correlated with grass cover. This result indicates that rainfall impact triggers more sediment delivery over vegetative barriers, but the influence weakens with increasing covers. A high cover can dissipate against more raindrop kinetic energy, which may explain the little effect of rainfall on sediment deposition for the 90% cover. *Ma et al.* [2013] and *Beuselinck et al.* [2002] also found that raindrop impact had the positive effect on sediment delivery on grass strips and on gentle plane slopes, respectively. These results imply that raindrop impact may strengthen sediment redetachment on bare soil slopes as well as on vegetated slopes [*Hairsine and Rose*, 1992]. It further indicates that the SDE values investigated in the absence of rainfall could be overestimated.

Introducing more inflow sediment, high inflow run led to a greater deposited sediment yield, but a smaller SDE compared with low inflow rate (Table 1). However, *Jin and Romkens* [2001] and *Le Bissonnais et al.* [2004] suggested that inflow discharge and sediment concentration had the minor effect on sediment deposition. The relationship between inflow discharge and sediment deposition would depend on not only

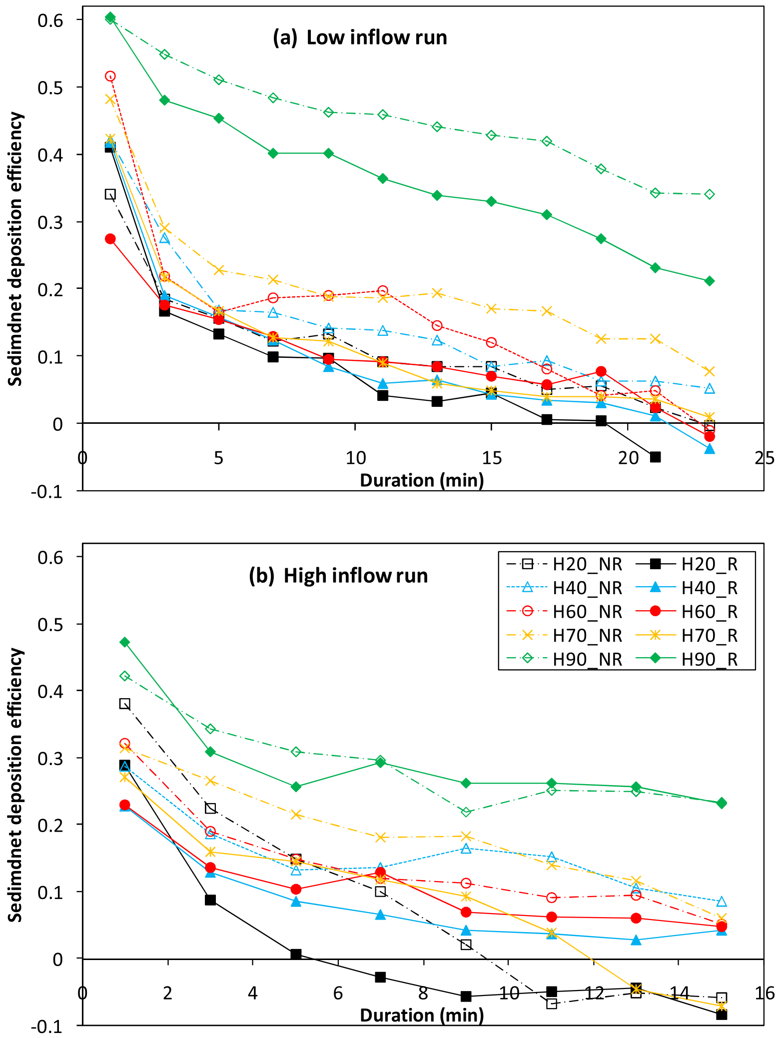

Figure 3. Sediment deposition efficiency (SDE) versus runoff duration for each test and the effect of rainfall.

runoff characteristics, but also particle or aggregate size distribution of inflow sediment. For a given vegetative strip, an increment in inflow discharge will increase runoff velocity and energy, which may trigger the delivery of more or coarser sediment. Consequently, the proportion of the triggered particle to all sediment would influence sediment deposition.

SDE gradually decreased with runoff duration, and it decreased more sharply at initial phase than at later stage of runoff (Figure 3). For the low-cover barriers impacted by raindrop, instantaneous SDE reached zero and even negative values (Figure 3). The appearance may derive from the redetachment of deposited sediment due to raindrop impact [*Hairsine and Rose*, 1992; *Salles et al*., 2000]. The continuously decreasing SDE with duration is in accord with a prevailing recognition [e.g., *Jin and Romkens*, 2001; *Le Bissonnais et al*., 2004; *Ma et al*., 2013], which hints that vegetative barriers will lose their efficiency in trapping inflow sediments at the later phase, and exist a sediment trapping capacity corresponding to the maximum deposited sediment yield for a given inflow [*Pan et al*., 2011].

3.2. Particle Selectivity of Deposited Sediments

SDE_{size} reflects the deposition characteristics of a given size sediment (equation (2)). Coarse particle had a greater SDE_{size} than fine sediment with the exception of <2 μm particle (Table 2). The exception is in line with some previous investigations. *Beuselinck et al*. [2002] found that <2 μm sediment had a smaller delivery rate than 2–8 μm particle over areas of net deposition. *Pan et al*. [2010] and *Ma et al*. [2013] also found

Table 2. Sediment Deposition Efficiency for Different Particle Sizes (SDE_{size}, Calculated by Equation (3)) for Each Test

Test	SDE	SDE_{size} for Different Particle Sizes (μm)				
		<2	2–10	10–25	25–50	>50
L20_NR	0.12	0.10	0.07	0.10	0.15	0.24
L20_R	0.08	0.01	0.03	0.05	0.19	0.31
L40_NR	0.14	0.07	0.03	0.07	0.35	0.48
L40_R	0.09	0.08	0.03	0.06	0.18	0.31
L60_NR	0.15	0.20	0.04	0.14	0.25	0.22
L60_R	0.10	0.23	0.00	0.07	0.15	0.20
L70_NR	0.20	0.27	0.13	0.19	0.25	0.24
L70_R	0.11	0.17	0.02	0.09	0.16	0.28
L90_NR	0.45	0.42	0.35	0.40	0.59	0.70
L90_R	0.36	0.34	0.27	0.32	0.50	0.58
H20_NR	0.08	0.08	0.05	0.04	0.13	0.29
H20_R	0.01	0.00	0.01	0.00	0.02	0.04
H40_NR	0.13	0.26	0.00	0.14	0.25	0.34
H40_R	0.09	0.04	0.03	0.11	0.14	0.10
H60_NR	0.16	0.11	0.07	0.19	0.27	0.39
H60_R	0.09	0.04	0.00	0.06	0.22	0.37
H70_NR	0.15	0.19	0.02	0.11	0.25	0.37
H70_R	0.10	0.02	0.07	0.10	0.16	0.18
H90_NR	0.29	0.36	0.10	0.21	0.45	0.55
H90_R	0.29	0.30	0.18	0.22	0.40	0.54

more sediment of <1 μm was subjected to deposition than that of 1–10 μm. This appearance may be attributed to the accumulative impact formation due to greater cohesive force between fine particles, rather than the runoff infiltration impact [*Ma et al*., 2013]. The >50 and 2–10 μm particles, respectively, corresponded to the maximum and minimum SDE_{size} values.

The ratio of SDE_{size} to SDE reflects particle selectivity of sediment deposition. For a given size particle, the ratio greater than 1.0 represents the particle easily deposited, and the ratio smaller than 1.0 represents the sediment particle easily transported. The average ratios of <2, 2–10, 10–25, 25–50, and >50 μm particles for all covers are 1.0, 0.4, 0.8, 1.7, and 2.4 (Figure 4), which indicates that the coarse particles of >25 μm are easily deposited over the grass barriers, and the <2 μm particles have a similar deposition characteristics to overall sediment. The easier deposition for the coarse (>25 μm) particles is in accord with the common recognition [e.g., *Jin and Romkens*, 2001; *Beuselinck et al*., 2002; *Han et al*., 2005]. *Ma et al*. [2013] also suggested that the coarse sediment (>40 μm) is easily deposited within plastic grass strips, and the fine particle of <1 μm had a greater SDE than 1–10 μm. The appearance disagrees with *Asadi et al*. [2007] who found that the fine (<1 μm) and large class (1–2 mm) particle had greater delivery rates at the occurrence of rill erosion. This implies that the deposited sediment would have a different particle selectivity from the eroded sediment.

SDE_{size} of each particle size increased with increasing grass covers (Table 2). For each size particle, there was a relatively small variability in the ratio of (SDE_{size}/SDE) among the 20–70% covers (Figure 4). However, compared with other covers, 90% cover had a smaller (SDE_{size}/SDE) ratio for coarse sediments, and a smaller variation coefficient in the ratio among different grain sizes (Figure 4). This indicates that the 90% cover barriers weaken the particle selectivity, and it may be related with the formation of backwater zone before the barriers. Backwater zone clearly retards flow velocity, and triggers more sediment deposition of relatively fine particles [*Hussein et al*., 2007; *Pan et al*., 2010].

Although raindrop impact generally decreased SDE (Table 1), it had no significant ($p = 0.05$) effect on the ratio of (SDE_{size}/SDE) (Figure 4). This indicates that raindrop impact decreases sediment deposition of all particle sizes, and does not influence particle selectivity of the deposited sediment. *Ma et al*. [2013] found that rainfall had no significant effect on particle size distribution of sediment deposited over simulated grass strips at 9–15° slopes, but it clearly triggered more coarse sediment (>50 μm) delivery at a 3° slope. The above results hint that the influence of rainfall on particle selectivity of deposited sediment may diminish with increasing slope gradients. As slopes increase, the gravity component of soil particle or aggregate along downslope direction increases and the sediment transport capacity of overland flow strengthens [*Savat*, 1977], and they may play a more important role in transporting sediment than the raindrop redetachment impact.

Due to the little effect of rainfall on particle selectivity, the relationships between SDE_{size} and SDE in the presence and absence of rainfall were scattered in Figure 5 and a linear equation could well fit them. Generally, the coarse particles corresponded to greater intercepts and slope gradients of the fitted lines than the fine particles except for <2 μm (Figure 5). Statistical analysis showed that there existed a difference in the intercept rather than slope gradient. This indicates that there is a relatively constant difference between SDE and SDE_{size}, which derives from particle sizes rather than vegetative strip characteristics.

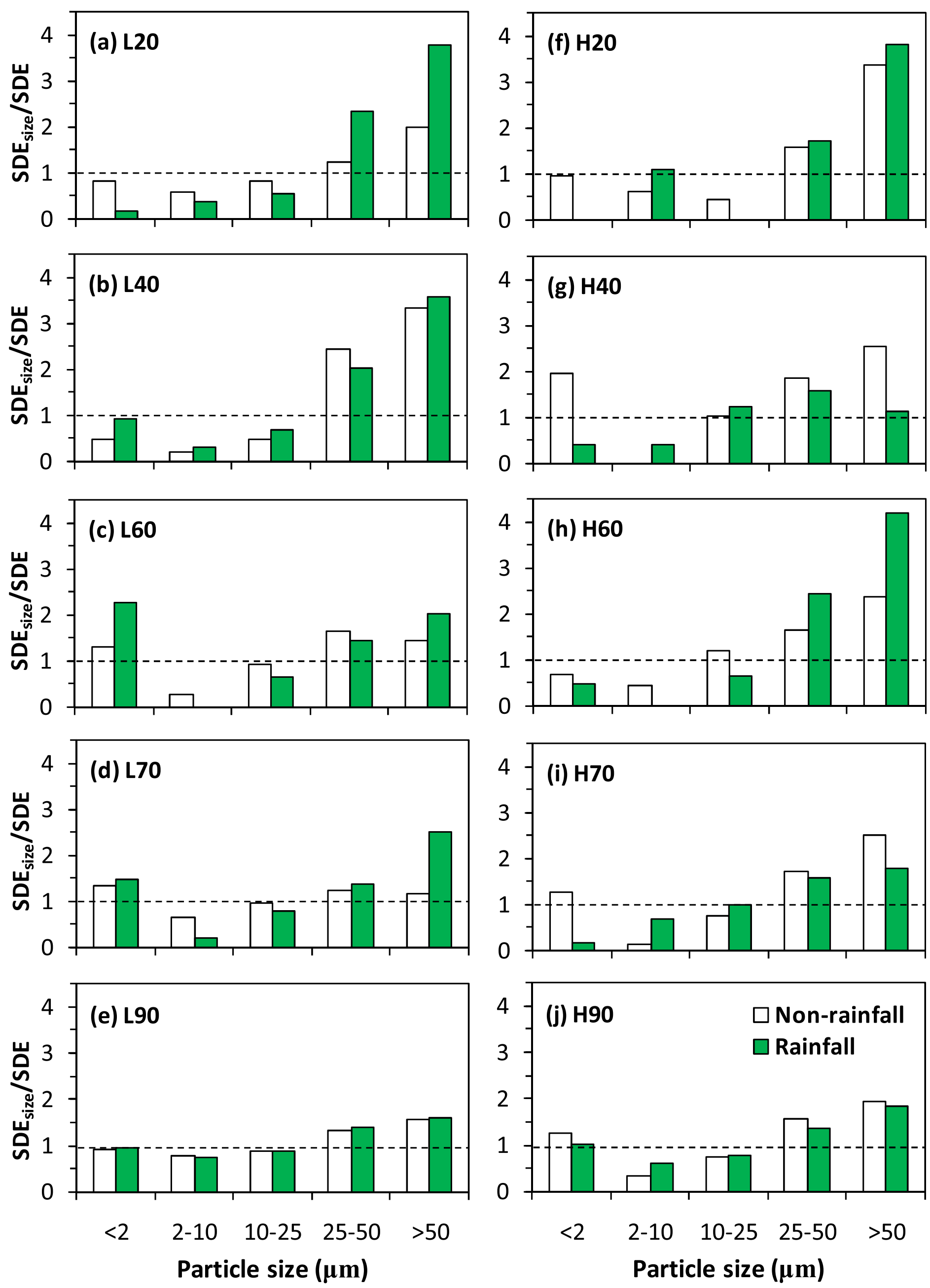

Figure 4. Particle selectivity of the deposited sediments (SDE_{size} is calculated by equation (3)).

There existed an interesting line for <2 μm particle: $SDE_{size} = 1.03SDE$, which almost overlaps 1:1 line (Figure 5). This indicates that clay soil (<2 μm) has a similar SDE to the tested loessial loam over grass barriers. *Pan et al.* [2010] also investigated the particle characteristics of deposited sediments on 5 m width grassed strips, and found a similar relationship between SDE_{size} and SDE to this study, and the clay soil (i.e., <2 μm) and 10–25 μm soil particles had a similar deposition efficiency to overall sediment. For the loamy soil in the loess plateau, the eroded sediment tended to have a greater clay fraction under rainfall conditions [*Zhang et al.*, 2011; *Wang et al.*, 2014]. The good performance of the grass barriers in trapping clay particles indicates that the nutrient loss from upslope cropland can remain within the vegetated slope since soil nutrient tends to be bounded onto fine particles [*Meyer et al.*, 1980; *Turnbull et al.*, 2010; *Zhang et al.*, 2011]. It deserves further investigations on how to strengthen the deposition of clay particle for the management of agricultural watersheds.

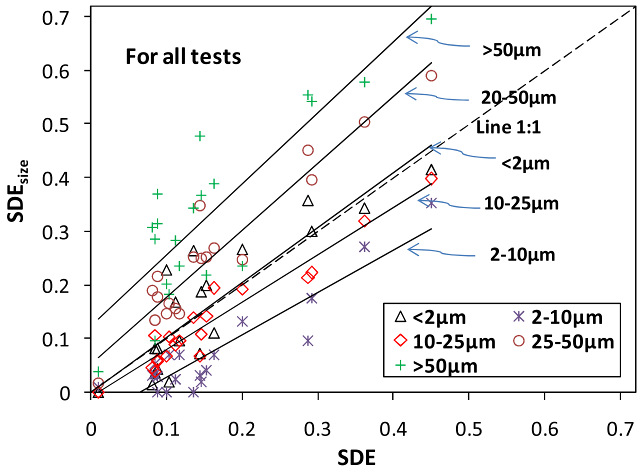

The regressed line equations

Size (μm)	SDE_{size}=*a* SDE+*b*			
	a	*b*	R^2	n
< 2	1.03	0.00	0.76**	20
2-10	0.79	-0.05	0.84**	20
10-25	0.88	-0.01	0.93**	20
25-50	1.25	0.05	0.91**	20
> 50	1.32	0.12	0.73**	20

** means significance at P=0.01 level.

Figure 5. The relationship between sediment deposition efficiency (SDE) and SDE_{size} for all tests.

The typical deposition processes of all particle sizes for the 40 and 90% covers were shown in Figure 6. Generally, each size fraction had a greater variability in deposition processes than overall sediment, especially for the low cover grass barriers. The greater variability may derive from the roll waves in overland flow on the low-cover slopes which can bring the periodical variation in water depth [*Zhang et al*., 2010]. For 90% cover, each size particle had a similar deposition process to overall sediment (Figures 6c and 6d). This indicates that for well vegetated strips, the deposited sediment has a similar particle size distribution during the runoff duration, although sediment deposition yield gradually decreases. This appearance does not agree with *Hairsine and Rose* [1992] who suggested sediment flux driven by runoff mainly depended on particle sizes on eroding slopes. It reminds that vegetative barriers may have a different sediment transport process from bare soil slopes.

3.3. Runoff Hydraulics

As grass covers increased from 20 to 90%, *Vs* decreased from 0.10 to 0.18 m s^{-1} for low inflow run, and from 0.12 to 0.23 m s^{-1} for high run (Figure 7). ANOVA showed that raindrop impact had no significant ($p = 0.05$) effect on *Vs* at the slope of 15°. This result is accord with the investigations of *Pan et al*. [2010] and *Ma et al*. [2013] on grassed slopes of 3–15°. These results disagree with the common recognition that raindrop impact retards overland flow velocity [*Savat*, 1977; *Kinnell*, 1991]. This discrepancy may be attributed to the steep slope and grass cover, and they compensate and weaken the raindrop impact on runoff momentum [*Guy et al*., 1990; *Ma et al*., 2013]. Raindrop impact significantly ($p = 0.05$) decreased the spatial variability in *Vs* on the whole grassed slope, since rainfall corresponded to a smaller variation coefficient than nonrainfall (0.20 versus 0.24 for all tests, Figure 7). This result indicates that rainfall impact may decrease the existence of maximum and minimum flow velocities to secure a flattened velocity distribution.

Vs decreased linearly with grass cover (*C*), and the linear equations of $Vs = 0.20–0.10C$ ($P < 0.01$, n = 10) and $Vs = 0.28–0.17C$ ($P < 0.01$, n = 10) were fitted for low and high inflow runs, respectively. As *C* increases from 0 to 1.0, the difference in the calculated *Vs* between the two lines decreases from 0.08 to 0.01 m s^{-1}. This indicates that the positive relation between inflow rate and *Vs* may diminish with increasing vegetation covers. The reason may due to the greater vegetative resistance due to inundated grass stems. Based on the fitted equations, *Vs* at $C = 0$ for low and high inflow runs is estimated to be 0.20 and 0.28 m s^{-1}, respectively, which will be used to calculate the bed resistance f_b.

The resistance *f* calculated using equation (9) increased with grass covers, and they were 2.65–20.3 and 2.86–24.3 for low and high inflow runs, respectively (Table 3). Inflow rates negatively related to *f*, and the exception of 90% cover may be attributed to the greater inundated water depth (7 mm versus 3 mm, Table 3) for high inflow run [*Lawrence*, 1997; *Pan et al*., 2016]. The additional resistance due to rainfall (f_r) was obtained as the resistance *f* in the presence of raindrop minus that in the absence rainfall. f_r on average accounted for 5 and 2% of *f* for low and high inflow runs, respectively, for all covers, and it had no relation with grass cover (Table 3). ANOVA also showed that raindrop impact had no significant effect on *f*.

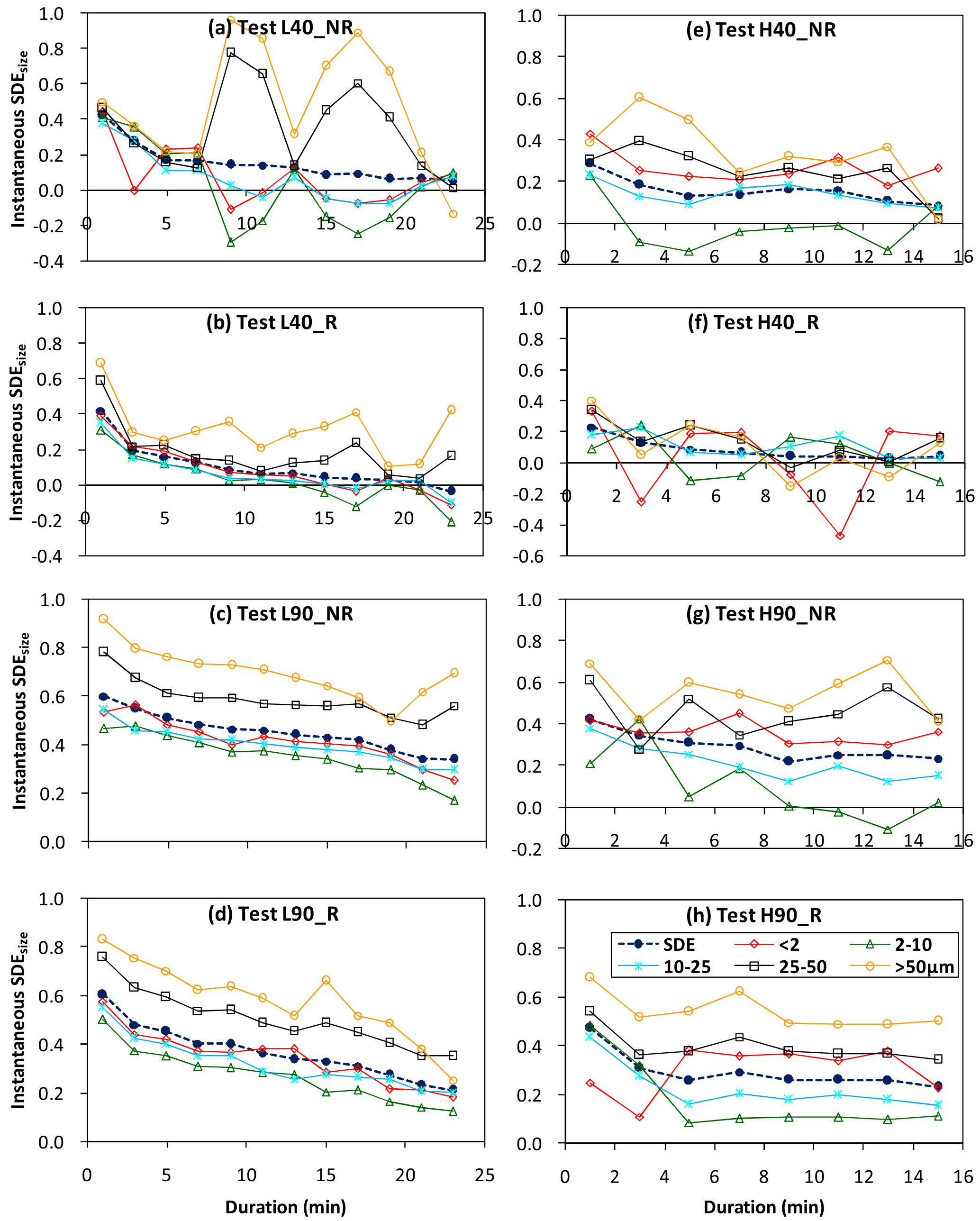

Figure 6. The deposition variation for different particle sizes with runoff duration for the typical (e.g., 40 and 90%) cover barriers under rainfall (R) and nonrainfall conditions.

The negligible f_r on the steep slope (15°) agrees with *Savat* [1977] who suggested that f_r diminished with increasing slope gradients, and it does not exceed 20% of total resistance for sheet laminar flows on gentle nonvegetated slopes.

For the grass plots, due to the negligible f_r, total resistance f can be expressed as the sum of resistance components derived from bed soil surface and grass cover/stems, respectively, i.e., $f = f_g + f_b$ [*Rauws*,1988; *Abrahams and Parsons*, 1994]. Assuming that f_b is equivalent to f on bare soil surface ($C = 0$), f_b were estimated to be 2.25 and 1.50 for low and high runs, respectively, based on the above calculated *Vs* values at $C = 0$. Consequently, the proportions of f_g to f were 15–85% and 44–94% for low and high runs, respectively, and they increased with increasing grass covers (Figure 8). The resistance partitioning for the 90% cover agrees with *Prosser et al.* [1995] who suggested that on a densely grassed surface more than 90% of flow resistance

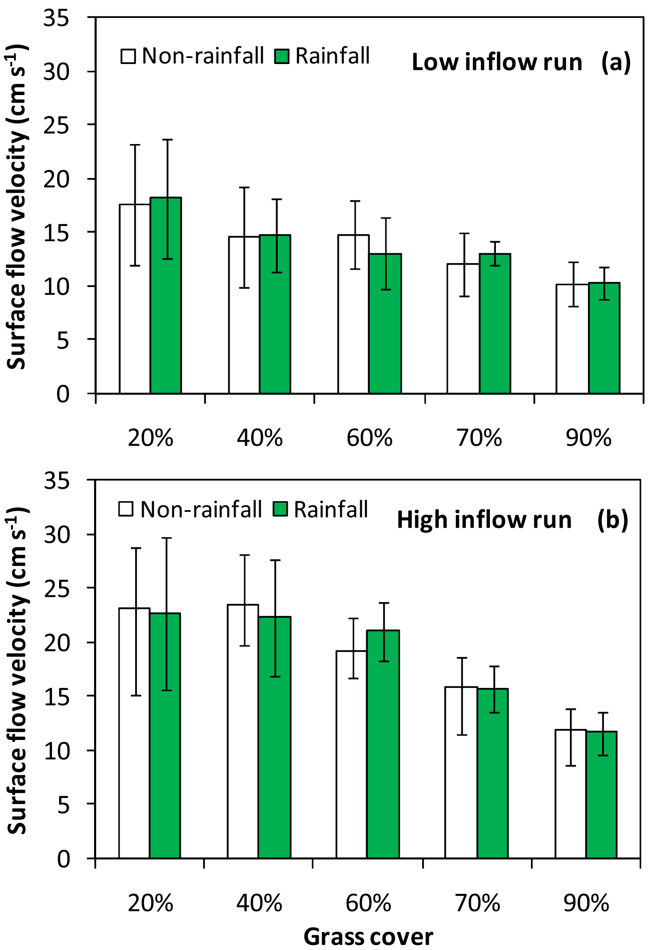

Figure 7. The measured surface flow velocity (*Vs*) for different grass covers and the effects of rainfall.

was exerted on plant stems. These results indicate that for high-cover slopes, grass cover will dissipate the majority of overland flow energy.

Unit stream powers (ω) calculated using equation (6) were approximately 0.6 and 1.3 J m^{-2} s^{-1} for low and high inflow runs, respectively (Table 3). The increment in runoff due to rainfall increased ω by 10%. No correlation existed between ω and *C*, implying that ω cannot effectively reflect the effect of grass cover on sediment deposition. This may derive from the resistance component due to grass stems, and the stream power dissipated against vegetation would have little relation with sediment transport. Therefore, ω_b directly impacting soil surface were calculated using equation (8) and listed in Table 3. The ω_b values were 0.09–0.52 and 0.09–0.75 J m^{-2} s^{-1} for low and high runs, respectively, and they decreased with increasing grass covers. Paired *t* test showed that raindrop impact had no significant ($p = 0.05$) effect on ω_b. The inflow rate had a positive effect on ω_b for low-cover barriers, and a negligible effect for high-cover ones (Table 1). This hints that for well-covered vegetated barriers, a increment

Table 3. Hydraulic Characteristics of Overland Flow for Different Grass Covers (ω_b and E_b, Respectively, Refer to Bed Stream Power and Rainfall Energy Directly Impacting Bed Soil Surface)

Test	Flow Rate (cm^2 s^{-1})	Mean Velocity *V* (cm s^{-1})	Water Depth (mm)	Hydraulic Resistance *f*	Stream Power ω (J m^{-2} s^{-1})	ω_b (J m^{-2} s^{-1})	$\omega_b + E_b$ (J m^{-2} s^{-1})
L20_NR	2.17	11.83	1.83	2.7	0.56	0.48	0.48
L40_NR	2.48	9.82	2.52	5.3	0.64	0.27	0.27
L60_NR	2.32	9.95	2.33	4.8	0.60	0.28	0.28
L70_NR	2.62	8.11	3.23	10.0	0.68	0.15	0.15
L90_NR	2.28	6.88	3.31	14.2	0.59	0.09	0.09
H20_NR	4.86	15.51	3.13	2.6	1.26	0.72	0.72
H40_NR	5.45	15.74	3.46	2.8	1.41	0.75	0.75
H60_NR	5.38	12.82	4.19	5.2	1.39	0.41	0.41
H70_NR	5.13	10.58	4.85	8.8	1.33	0.23	0.23
H90_NR	5.00	7.93	6.30	20.3	1.29	0.10	0.10
L20_R	2.61	12.20	2.14	2.9	0.67	0.52	0.72
L40_R	2.54	9.92	2.56	5.3	0.66	0.28	0.43
L60_R	2.44	8.78	2.78	7.3	0.63	0.19	0.29
L70_R	2.81	8.79	3.19	8.4	0.73	0.20	0.27
L90_R	2.40	6.94	3.46	14.6	0.62	0.10	0.12
H20_R	5.26	15.18	3.46	3.0	1.36	0.68	0.98
H40_R	4.72	14.95	3.16	2.9	1.22	0.65	0.88
H60_R	5.98	14.13	4.23	4.3	1.55	0.54	0.70
H70_R	5.12	10.55	4.85	8.8	1.32	0.23	0.34
H90_R	5.77	7.83	7.36	24.3	1.49	0.09	0.13

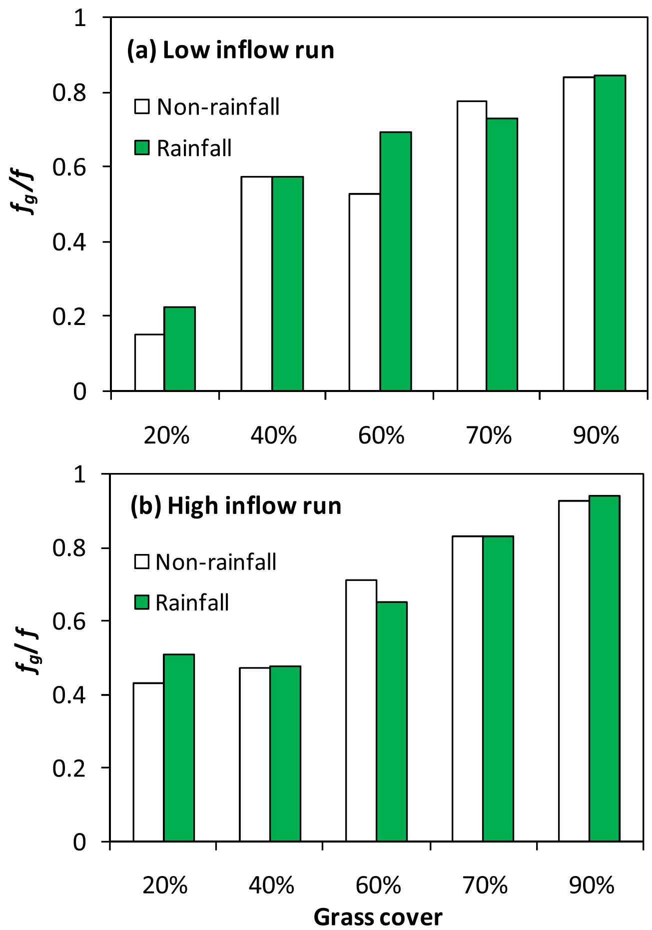

Figure 8. The resistance contribution derived from grass plantation (f_g) to total resistance (f) for different cover barriers.

in runoff rate may not result in a greater energy dissipated against bed soil surface.

3.4. Relationship Between Hydraulics and Sediment Deposition

3.4.1. Flow Velocity and Sediment Deposition

Due to a similar total runoff volume for high and low runs (Table 1), the experimental data of all trials were used to analyze the relationship between sediment deposition and flow hydraulics. SDE decreased with flow velocity (V) by a power function, i.e., SDE $= aV^{-b}$, and there was a significant difference ($p = 0.05$) in the regressed equations between the absence and presence of rainfall (Figure 9a). The equations were converted to linear expressions by taking logarithms to analyze the difference derived from rainfall. Covariance analysis showed that rainfall significantly ($p = 0.05$) decreased the intercept, and did not influence the slope gradient of the logarithmic lines. This implies that rainfall impact alters the relationship between sediment delivery and overland flow hydraulics for vegetative barriers.

The difference in SDE between the presence and absence of rainfall increased with flow velocities (Figure 9a). This indicates that an increment in vegetative cover (C) may diminish the effect of rainfall on sediment deposition since flow velocity is inversely related to the cover (Figure 7). It may be attributed to two reasons, one is that a increasing C decreases the raindrop kinetic energy directly impacting soil surface; another is that a increasing C retards flow velocity and increases water depth, and the increased water depth weakens the impact of raindrop [*Savat*, 1977].

Spatial distribution in overland flow has an important effect on soil erosion and sediment transport [*Abrahams et al*., 1991; *Smith et al*., 2011], so standard deviation in *Vs* for each trail was calculated and used to discuss the sediment deposition (Figure 9b). SDE decreased with increasing standard deviations by a power function, which means that the existence of concentrated flow lines will decrease sediment deposition over vegetative barriers. This result agrees with *Walsh et al*. [1997] and *Blanco-Canquia et al*. [2004] who found that more sediments were trapped over vegetated strips for flat sheet flow than concentrated flow. Additionally, both flow velocity and its standard deviation were used to predict SDE for all covers. However, analysis of stepwise linear regression after taking logarithm showed that standard deviation could not enter the model. This implies that the effect of rainfall on SDE cannot be reflected by the spatial heterogeneity in flow velocity.

3.4.2. Stream Power and Sediment Deposition

For all tests, SDE significantly ($p = 0.05$) related with bed stream power (ω_b), rather than unit stream power (ω). This result indicates that sediment deposition may be mainly dominated by the energy dissipated against soil surface, rather than total stream energy for vegetated barriers. A power function well described the relation between SDE and ω_b, and rainfall impact brought about a smaller SDE value (Figure 10a).

For the grassed slopes, rainfall kinetic energy E can be divided into the components impacting grass cover (E_g) and bed soil surface (E_b), respectively. Due to the interception and buffer impacts of grass cover on raindrop

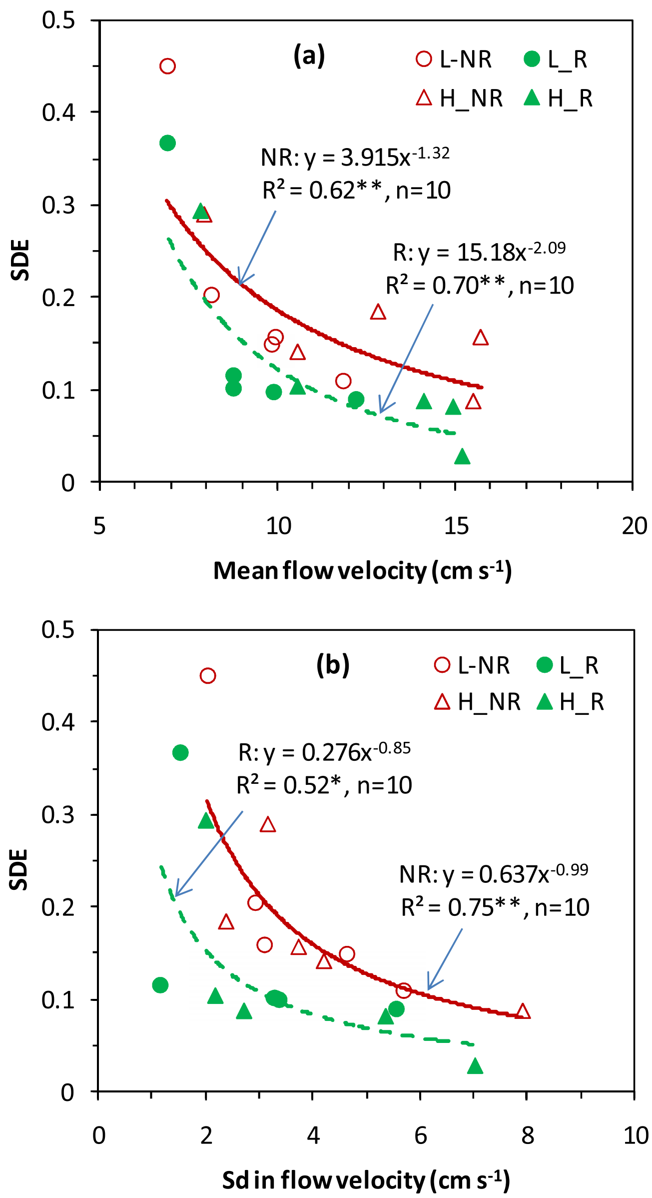

Figure 9. The relationship between SDE and (a) flow velocity and (b) its standard variation (SD) and the effects of rainfall (* and ** represents significance at $p = 0.05$ and $p = 0.01$, respectively).

falling velocity, E_b was mainly used to investigate the rainfall impact on sediment deposition. E_b was calculated as E multiplying (1-C). Correspondingly, as grass cover (C) increased from 20 to 90%, the E_b values for 60 and 90 mm h^{-1} rainfall intensities decreased linearly from 0.2 to 0.025 J m^{-2} s^{-1} and from 0.31 to 0.04 J m^{-2} s^{-1} according to the simulated rainfall characteristics [*Wang et al.*, 2005] (Table 1).

Since E_b and ω_b had a same dimension, their sum was further used to predict SDE (Table 3 and Figure 10b). Due to the additional E_b, the regressed curves in the presence and absence of rainfall (Figure 10b) were almost overlapped compared with Figure 10a. This highlights the importance of rainfall kinetic energy to sediment deposition, and expands the impact of raindrop redetachment on deposited sediments over vegetated barriers [*Salles et al.*, 2000]. Both raindrop kinetic energy and stream power available for surface soil contributed to the sediment deposition in the net deposition area of the grass barriers. However, *Martinez-Mena et al.* [2000] suggested that raindrop impact was the predominant contributor to soil loss for the vegetated plot. This difference implies that the dynamics of sediment transport on vegetated slopes may alter with the predominant erosion pattern of detachment or deposition.

From the equation fitted by all data, SDE will be negligible when ($E_b + \omega_b$) exceeds 5.0 (Figure 10b). A greater ($E_b + \omega_b$) value may correspond to lower vegetative covers, greater flow discharge or rainfall intensity which trigger soil erosion occurrence. In other words, the relationship between SDE and ($E_b + \omega_b$) would lose its efficacy over areas of non-net deposition.

For all grass covers, due to the synchronism of inflow rate and rainfall (i.e., high inflow rate corresponding to a high rainfall intensity), the ratios of E_b to ω_b varied from 0.26 to 0.52 and from 0.28 to 0.51 for low and high inflow runs, respectively. The ratio for each grass cover was relatively constant with an average of 0.41. This implies that an increase in grass cover synchronously decreases the energies of rainfall and runoff dissipated against sediment delivery, and it would be helpful to model sediment transport on vegetated slopes as a function of vegetation cover. The average value of 0.41 may partly reflect the relative contribution of rainfall to sediment delivery compared with runoff transport under the experimental conditions.

The close relationship between SDE and ($\omega_b + E_b$), as well as the greater deposition efficiency for coarse (>25 μm) sediments hints that sediment movements in saltation or bed load driven by either overland runoff and/or rainfall mainly control sediment deposition over vegetated barriers. This agrees with *Asadi et al.* [2007, 2011]

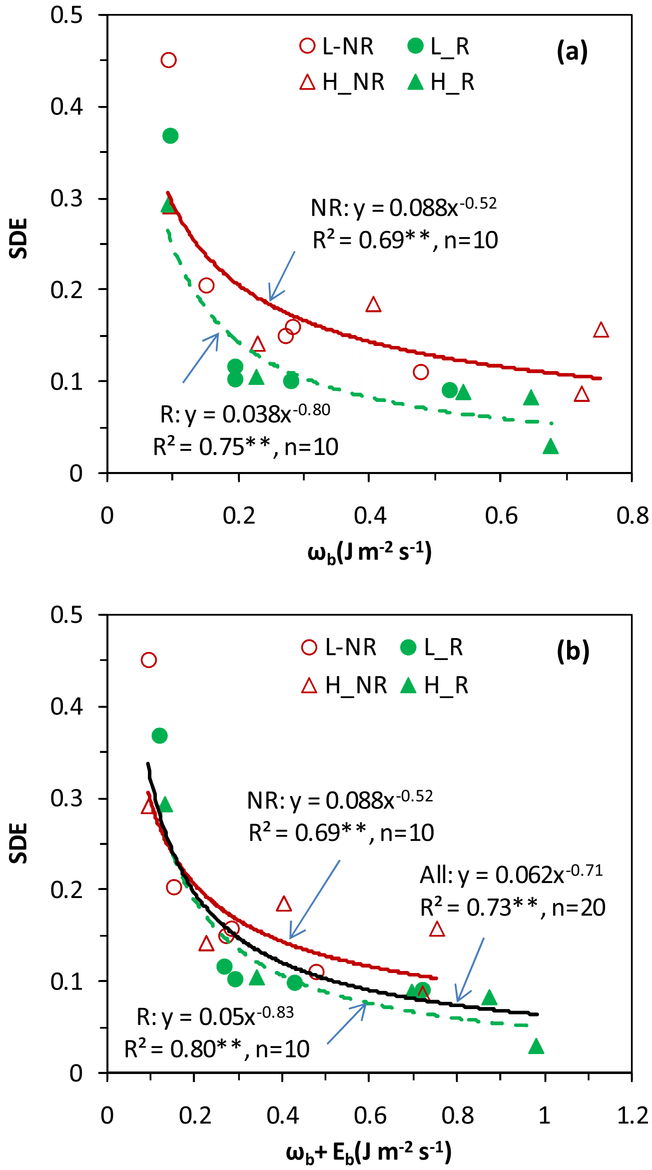

Figure 10. The relationship between SDE and (a) bed stream power (ω_b) and (b) ($\omega_b + E_b$) and the effect of rainfall (ω_b and E_b refer to unit stream power and rainfall kinetic energy directly impacting soil surface, respectively; and ** represents significance at $p = 0.01$).

who suggested that when the stream power exceeded 0.1–0.15 J m^{-2} s^{-1} bed load movement became the dominant transport mechanism under flow-driven condition.

4. Conclusion

The steep cropland has been widely transformed into grassland in the loess hilly region of China in recent years. The experiments on grass barriers with different grass covers were conducted to focus on the effectiveness of regrassed steep slope in controlling sediment eroded from upslope cropland.

The considerable inflow sediment was deposited within the grass barriers on the 15° slope, which indicates that the mode of revegetation of steep cropland in the "Grain for Green" project is effective. When being subjected to greater storms, the grass barriers had greater deposited sediment yield. The deposition order of sediment particle size (μm) followed (>50) $>$ (25–50) $>$ (10–25) $=$ (<2) $>$ (2–10). The greater deposition in clay can help to reduce the loss of cropland nutrient into surface waters. As the grass covers increased, sediment deposition strengthened while the particle selectivity weakened. Raindrop impact significantly decreased the deposited sediment yield, and the percentage of reduction increased from 10 to 60% with increasing grass covers. However, rainfall had little effect on the particle selectivity of deposited sediment.

The 20–90% grass cover contributed to 30–90% of the total resistance to overland flow, suggesting that grass cover almost mirrors an increment in resistance. The raindrop impact had little effect on *Vs* and hydraulic resistance for all grass covers. Sediment deposition correlated with flow velocity and the spatial distribution of overland flow, but they cannot explain the negative effect of rainfall impact on sediment deposition. Both stream power and rainfall kinetic energy impacting bed soil surface contributed to sediment deposition on the net deposition area of grass strips. These results suggest that raindrop impact increases sediment transport capacity for overland flow, and the influence mainly depends on rainfall kinetic energy, rather than an alteration in overland flow hydraulics.

Notation

SDE	sediment deposition efficiency (for all particle sizes), the ratio of deposited to inflow sediment.
SDE_{size}	SDE for a given particle size (e.g., $<2\mu$m), calculated by equation (3).

SDR	sediment delivery rates (for all particle sizes) (g s^{-1}).
SDR_{inflow}	SDR in the inflow (g s^{-1}).
$SDR_{outflow}$	SDR in the outflow (g s^{-1}).
SDR''_{inflow}	SDR for a given particle size in the inflow (g s^{-1}).
$SDR''_{outflow}$	SDR for a given particle size in the outflow (g s^{-1}).
R (rainfall)	tests conducted in the presence of rainfall.
NR (nonrainfall)	tests conducted in the absence of rainfall.
L (low)	tests subjected to low inflow rate and rainfall intensity.
H (high)	tests subjected to high inflow rate and rainfall intensity.
C	grass cover (e.g., 20%).
S	slope steepness (m m^{-1}).
q	flow rate per unit width (m^2 s^{-1}).
Vs	surface flow velocity (m s^{-1}).
V	mean flow velocity (m s^{-1}).
h	water depth (m), $h = q/V$.
E	rainfall kinetic energy (J m^{-2} s^{-1}).
E_g	E directly impacting grass cover, calculated as E multiplying grass cover C.
E_b	E directly impacting bed soil surface.
f	Darcy-Weisbach resistance coefficient to overland flow for a grassed plot.
f_r	resistance component due to raindrop impact.
f_g	resistance component derived from grass stems and leaves.
f_b	resistance component derived from bed surface, corresponding to bare soil surface ($C = 0$).
τ	shear stress (N m^{-2}), $\tau = \tau_b + \tau_g$.
τ_b	τ impacting bed soil surface.
τ_g	τ impacting grass stems and leaves.
ω	unit stream power (J m^{-2} s^{-1}).
ω_b	ω dissipated against bed soil surface.
ω_g	ω dissipated against grass stems/leaves.

Acknowledgments
This research was jointly funded by the National Natural Science Foundation of China Project (grants 41271285, 51309007, and 41530858), and the Fundamental Research Funds for the Central Universities (2015KJJCA08). The experimental data are partly listed in the tables in the manuscript; any additional data may be obtained from C. Z. Pan (e-mail: pancz@bnu.edu.cn). The authors would like to express deep gratitude to the reviewers for their constructive comments and helpful suggestions on the manuscript.

References

Abrahams, A. D., and A. J. Parsons (1994), Hydraulics of interrill overland flow on stone-covered desert surfaces, *Catena*, *23*, 111–140.
Abrahams, A. D., A. J. Parsons, and S. H. Luk (1991), The effect of spatial variability in overland flow on the downslope pattern of soil loss on a semi-arid hillslope, southern Arizona, *Catena*, *18*, 255–270.
Asadi, H., H. Ghadiri, C. W. Rose, B. Yu, and J. Hussein (2007), An investigation of flow-driven soil erosion processes at low streampowers, *J. Hydrol.*, *342*, 134–142.
Asadi, H., A. Moussavi, H. Ghadiri, and C.W. Rose (2011), Flow-driven soil erosion processes and the size selectivity of sediment, *J. Hydrol.*, *406*, 73–81.
Bagnold, R. A. (1966), An approach to the sediment transport problem from general physics, U. S. Geol. Surv. Prof. Pap., 422-I, 1-I37.
Beuselinck, L., G. Govers, P. B. Hairsine, G. C. Sander, and M. Breynaert (2002), The influence of rainfall on sediment transport by overland flow over areas of net deposition, *J. Hydrol.*, *257*, 145–163.
Blanco-Canqui, H., C. J. Gantzerb, S. H. Andersonb, E. E. Albertsc, and A. L. Thompsond (2004), Grass barrier and vegetative filter strip effectiveness in reducing runoff, sediment, nitrogen, and phosphorus loss, *Soil Sci. Soc. Am. J.*, *68*, 1670–1678.
Cerdà, A. (1998a), Soil aggregate stability under different Mediterranean vegetation types, *Catena*, *32*, 73–86.
Cerdà, A. (1998b), The influence of aspect and vegetation on seasonal changes in erosion under rainfall simulation on a clay soil in Spain, *Can. J. Soil Sci.*, *78*(2), 321–330.
Deng, L., Z. P. Shangguang, and R. Li (2012), Effects of the grain-for-green programme on soil erosion in China, *Int. J. Sediment Res.*, *27*, 120–127.
Flanagan, D. C., and M. A. Nearing (2000), Sediment particle sorting on hillslope profiles in the WEPP model, *Trans. ASAE*, *43*(3), 573–583.
Gumiere, S. J., Y. L. Bissonnais, D. Raclot, and B. Cheviron (2011), Vegetated filter effects on sedimentological connectivity of agricultural catchments in erosion modelling: A review, *Earth Surf. Processes Landforms*, *36*, 3–19.
Guy, B. T., W. T. Dickinson, R. P. Rudra, and G. J. Wall (1990), Hydraulics of sediment-laden sheet flow and the influence of simulated rainfall, *Earth Surf. Processes Landforms*, *15*, 101–118.
Hairsine, P. B., and C. W. Rose (1992), Modeling water erosion due to overland flow using physical principles: 1. Sheet flow, *Water Resour. Res.*, *28*(1), 237–243.
Hairsine, P. B., L. Beuselinck, and G. C. Sander (2002), Sediment transport through an area of net deposition, *Water Resour. Res.*, *38*(6), 221–227, doi:10.1029/2001WR000265.
Han, J., J. S. Wu, and A. Craig, (2005), Suspended sediment removal by vegetative filter strip treating highway runoff, *J. Environ. Sci. Health Part A*, *40*(8), 1637–1649.
Horton, R. E., H. R. Leach, and R. Van Vliet (1934), Laminar sheet-flow, *Trans. Am. Geophys. Union*, *15*, 393–404.

Hussein, J., B. Yu, H. Ghadiri, and C. Rose (2007), Prediction of surface flow hydrology and sediment retention upslope of a vetiver buffer strip, *J. Hydrol.*, *338*, 261–272.

Jiang, D. S. (1997), *Soil Loss and its Controlling Mode on the Loess Plateau*, China's Water Conserv. and Hydropower Press, Beijing.

Jin, C. X., and M. J. M. Romkens (2001), Experimental studies of factors in determining sediment trapping in vegetative filter strips, *Trans. ASAE*, *44*(2), 277–288.

Kinnell, P. I. A. (1991), The effect of flow depth on sediment transport induced by raindrops impacting shallow flows, *Trans. ASAE*, *34*, 161–168.

Lawrence, D. S. L. (1997), Macroscale surface roughness and frictional resistance in overland flow, *Earth Surf. Processes Landforms*, *22*(4), 365–382.

Le Bissonnais, Y., V. Lecomte, and O. Cerdan (2004), Grass strip effects on runoff and soil loss, *Agronomie*, *24*, 129–136.

Liu, X. M., X. Y. Zhang, and M. H. Zhang (2008), Major factors influencing the efficacy of vegetated buffers on sediment trapping: a review and analysis, *J. Environ. Qual.*, *37*, 1667–1674.

Ma, L., C. Z. Pan, Y. G. Teng, and Z. P. Shangguan (2013), The performance of grass filter strips in controlling high-concentration suspended sediment from overland flow under rainfall/non-rainfall conditions, *Earth Surf. Processes Landforms*, *38*, 1523–1534.

Malam Issa, O., Y. Le Bissonnais, O. Planchon, D. Favis-Mortlock, N. Silvera, and J. Wainwright (2006), Soil detachment and transport on field- and laboratory-scale interrill areas: Erosion processes and the size-selectivity of eroded sediment, *Earth Surf. Processes Landforms*, *31*, 929–939.

Martinez-Mena, M., J. Alvarez Rogel, J. Albaladejo, and V. M. Castillo (2000), Influence of vegetal cover on sediment particle size distribution in natural rainfall conditions in a semiarid environment, *Catena*, *38*(3), 175–190.

Martinez-Mena, M., V. M. Castillo, and J. Albaladejo (2002), Relations between interrill erosion processes and sediment particle size distribution in a semiarid Mediterranean area of SE of Spain, *Geomorphology*, *45*, 261–275.

Meyer, L. D., W. C. Harmon, and L. L. McDowell (1980), Sediment size eroded from crop row sideslopes, *Trans. ASAE*, *23*, 891–898.

Morgan, R. P. C., J. N. Quinton, R. E. Smith, G. Govers, J. W. A. Poesen, K. Auerswald, G. Chisci, D. Torri, and M. E. Styczen (1998). The European Soil Erosion Model (EUROSEM): A dynamic approach for predicting sediment transport from fields and small catchments, *Earth Surf. Processes Landforms*, *23*, 527–544.

Novara, A., L. Gristina, F. Guaitoli, A. Santoro, and A. Cerdà (2013), Managing soil nitrate with cover crops and buffer strips in Sicilian vineyards, *Solid Earth*, *4*, 255–262, doi:10.5194/se-4-255-2013.

Palacio, R. G., A. J. Bisigato, and P. J. Bouza (2014), Soil erosion in three grazed plant communities in Northeastern Patagonia, *Land Degrad. Dev.*, *25*(6), 594–603.

Pan, C., L. Ma, J. Wainwright, and Z. Shangguan (2016), Overland flow resistances on varying slope gradients and partitioning on grassed slopes under simulated rainfall, *Water Resour. Res.*, *52*, 2490–2512, doi:10.1002/2015WR018035.

Pan, C. Z., and Z. P. Shangguan (2006), Runoff hydraulic characteristics and sediment generation in sloped grassplots under simulated rainfall conditions, *J. Hydrol.*, *331*, 178–185.

Pan, C. Z., Z. P. Shangguan, and T. W. Lei (2006), Influences of grass and moss on runoff and sediment yield on sloped loess surfaces under simulated rainfall, *Hydrol. Processes*, *20*, 3815–3824.

Pan, C. Z., L. Ma, and Z. P. Shangguan (2010), Effectiveness of grass strips in trapping suspended sediments from runoff, *Earth Surf. Processes Landforms*, *35*, 1006–1013.

Pan, C. Z., L. Ma, Z. P. Shangguan, and A. Z Ding (2011), Determining the sediment trapping capacity of grass filter strips, *J. Hydrol.*, *405*, 209–216.

Parsons, A. J., A. D. Abrahams, and J. Wainwright (1994), Rainsplash and erosion rates in an interrill area on semi-arid grassland, Southern Arizona, *Catena*, *22*(3), 215–226.

Prosser, I. P., W. E. Dietrich, and J. Stevenson (1995), Flow resistance and sediment transport by concentrated overland flow in a grassland valley, *Geomorphology*, *13*, 71–86.

Rauws, G. (1988), Laboratory experiments on resistance to overland flow due to composite roughness, *J. Hydrol.*, *103*, 37–52.

Salles, C., J. Poesen, J., and G. Govers (2000), Statistical and physical analysis of soil detachment by raindrop impact: Rain erosivity indices and threshold energy, *Water Resour. Res.*, *36*(9), 2721–2729.

Savat, J. (1977), The hydraulics of sheet flow on a smooth surface and the effect of simulated rainfall, *Earth Surf. Processes Landforms*, *2*, 125–140.

Shi, Z. H., N. F. Fang, F. Z., Wu, L. Wang, B. J. Yue, and G. L. Wu (2012), Soil erosion processes and sediment sorting associated with transport mechanisms on steep slopes, *J. Hydrol.*, *454*, 123–130.

Smith, M. W., N. J. Cox, and L. J. Bracken (2011), Terrestrial laser scanning soil surfaces, a field methodology to examine soil surface roughness and overland flow hydraulics, *Hydrol. Processes*, *25*, 842–860.

Tang, K. L., K. L. Zhang, and A. L. Lei (1998), Critical slope gradient for compulsory abandonment of farmland on the hilly Loess Plateau, *Chin. Sci. Bull.*, *43*, 409–412.

Turnbull, L., J. Wainwright, and R. E. Brazier (2010), Hydrology, erosion and nutrient transfers over a transition from semi-arid grassland to shrubland in the South-Western USA: A modelling assessment, *J. Hydrol.*, *388*, 258–272.

Wainwright, J. (2009), Desert ecogeomorphology, in *Geomorphology of Desert Environments*, edited by A. J. Parsons and A. D. Abrahams, 2nd ed., pp. 21–66, Springer, Berlin.

Wainwright, J., A. J. Parsons, E. N. Mueller, R. E. Brazier, M. Powell, and B. Fenti (2008), A transport-distance approach to scaling erosion rates: 1. Background and model development, *Earth Surf. Processes Landforms*, *33*, 813–826.

Walsh, P. M., M. E. Barrett, J. F. Malina, and R. J. Charbeneau (1997), *Use of Vegetative Controls for Treatment of Highway Runoff*, Cent. for Res. in Water Resour., Univ. of Tex. at Austin, Austin.

Wang, L., Z. H. Shi, J. Wang, N. F. Fang, and D. Wang (2014), Rainfall kinetic energy controlling erosion processes and sediment sorting on steep hillslopes: A case study of clay loam soil from the Loess Plateau, China, *J. Hydrol.*, *512*, 168–176.

Wang, Z. L., Q. M. Sun, F. L. Zheng, and Z. H. Niu (2005), Physically-based model of rainfall flow kinetic energy [in Chinese with English abstract], *J. Hydraul. Eng. China*, *36*(11), 1280–1285.

Xu, X. Z., D. Q. Liu, H. W. Zhang, Z. D. Dong, and M. D. Zhu (2006), Laboratory rainfall simulation with controlled rainfall intensity and drainage [in Chinese with English abstract], *J. Beijing Forestry Univ.*, *28*(5), 52–58.

Zhang, G. H., R. T. Luo, Y. Cao, R. Shen, and X. C. Zhang (2010), Correction factor to dye measured flow velocity under varying water and sediment discharges, *J. Hydrol.*, *389*, 205–213.

Zhang, G. H., G. B. Liu, G. L. Wang, and Y. X. Wang (2011), Effects of vegetation cover and rainfall intensity on sediment-bound nutrient loss, size composition and volume fractal dimension of sediment particles, *Pedosphere*, *21*(5), 676–684.